Electronic Supplementary Material (ESI) for New Journal of Chemistry.

Multichannel transport conjugated polymers based on through-space naphthalene

Meijing Li[a,b†], Xinxin Zhang[b†], Shijie Zhen[a*], Jingkun Xu[b,c*],

[a] State Key Laboratory of Luminescent Materials and Devices, South China University of Technology, Guangzhou 510640, China

[b] School of Pharmacy, Jiangxi Science & Technology Normal University, Nanchang 330013, China

[c] College of Chemistry and Molecular Engineering, Qingdao University of Science & Technology, Qingdao, 266042, China

[†] These authors contributed equally to this work

Experimental section

^{1}H and ^{13}C nuclear magnetic resonance (NMR) spectra were recorded on a Bruker DRX 500 spectrometer at 500 MHz, using deuterated chloroform as solvent with tetramethylsilane (TMS) as a reference. TGA were performed on a Netzsch TG 209 at a heating rate of 10 ^{o}C/min under a nitrogen flow. The DSC was measured on a Netzsch DSC 204 under nitrogen flow at a heating rate of 10 ^{o}C min^{-1}. UV-vis absorption and PL spectra were recorded on a Shimadzu UV-3600 spectrometer and a HORIBA scientific fluoromax-4 spectra-fluorometer, respectively. PL quantum yields were measured using an IS080 LabSphere integrating sphere with excitation by a 325 nm HeCd laser (MellesGriot). CV data were measured on a CHI800C electrochemical workstation equipped with a graphite working electrode, a saturated calomel electrode as the reference electrode, a Pt sheet counter electrode, and carried out with anhydrous dichloromethan under an argon atmosphere, with tetrabutylammonium hexa-fluorophosphate as the supporting electrolyte. Therefore, the HOMO and LUMO energy levels were obtained from the equation $E_{HOMO} = -(E_{ox} + 4.4)$ eV and E_{LUMO} = (HOMO + E_g) eV.

Materials

Commercially available reagents were used without further purification. 1,8-dibromonaphthalene, 1,4-dibromonaphthalene，1,5-dibromonaphthalene, thiophene, 2,3-dihydrothieno[3,4-*b*][1,4]dioxine, and tetrakis(triphenylphosphine)palladium(0) ($Pd(PPh_3)_4$) were purchased from energy chemistry. Ar-$SnBu_3$ (Th-$SnBu_3$, EDOT-$SnBu_3$) was synthesized according to previous reports.[1]

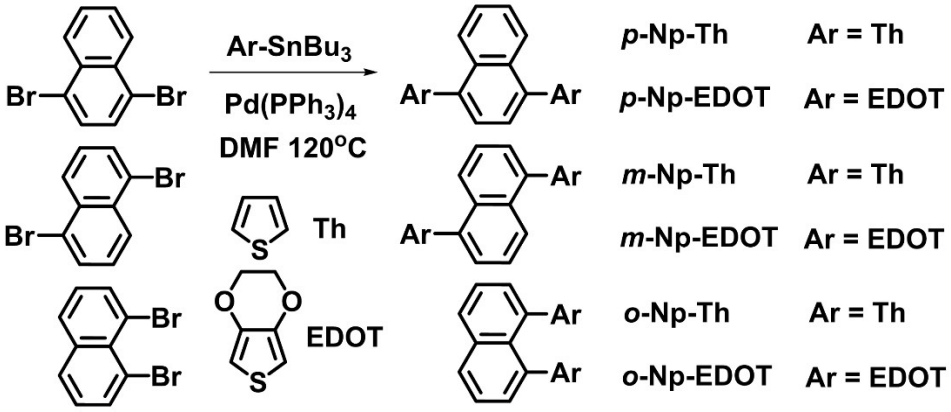

Fig. S1 The synthetic routes toward oligomers based on naphthalene.

1,8-Di(thiophen-2-yl)naphthalene (*o*-Np-Th): 1,8-dibromonaphthalene (100 mg, 0.35 mmol), tributyl(thiophen-2-yl)stannane (391.8 mg, 1.05 mmol), $Pd(PPh_3)_4$ (40.44 mg, 0.035 mmol) and DMF (20 mL) were added a two-necked bottle (50 mL). The mixture was heated to 120 ^oC for 12 h under nitrogen. The reaction solution was cooled to the temperature and slowly poured into 300 mL ice water, extracted with 100 mL $CHCl_2$, washed three times with saturated sodium chloride solution and dried over $MgSO_4$. After removal of the organic solvent, the crude product was purified by silica chromatography to give a faint yellow solid with yield of 84 mg (82%). ^1H NMR (500 MHz, $CDCl_3$), δ (TMS, ppm): 7.95–7.93 (m, 2H), 7.61–7.59 (m, 2H), 7.55–7.52 (m, 2H), 7.04–7.03 (m, 2H), 6.65–6.63 (m, 2H), 6.49–6.48 (m, 2H). ^{13}C NMR (125 MHz, $CDCl_3$) δ 144.20, 135.44, 132.50, 132.39, 130.60, 129.24, 127.67, 126.77, 125.12, 123.99. HRMS ($C_{18}H_{12}S_2$): *m/z* 293.88 (M^+, calcd 292.03).

The procedure of the **1,4-di(thiophen-2-yl)naphthalene (*p*-Np-Th)** were similar to that describe for *o*-Np-Th, the white needle crystal of *p*-Np-Th was obtained with yield of 78.1%. ^1H NMR (500 MHz, $CDCl_3$), δ (TMS, ppm): 8.31-8.29 (m, 2H), 7.60 (s, 2H), 7.54–7.52 (m, 2H), 7.47–7.46 (m, 2H), 7.29–7.28 (m, 2H), 7.23–7.21 (m, 2H). ^{13}C NMR (125 MHz, $CDCl_3$) δ 141.58, 132.73, 132.29, 127.63, 127.57, 127.42, 127.33, 126.49, 126.36, 126.18, 125.83. HRMS ($C_{18}H_{12}S_2$): *m/z* 293.88 (M^+, calcd 292.03).

The produce of the **1,5-di(thiophen-2-yl)naphthalene (*m*-Np-Th)** were similar to that describe for *o*-Np-Th The white needle crystal of *m*-Np-Th with yield of 78.9%. ^1H NMR (500 MHz, $CDCl_3$), δ (TMS, ppm): 8.25(d, *J* = 10.95 Hz, 2H), 7.61 (d, *J* = 8.65 Hz, 2H), 7.51–7.44 (m, 4H), 7.26–7.25 (m, 2H), 7.21–7.19 (m, 2H). ^{13}C NMR (125 MHz, $CDCl_3$) δ 141.83, 132.45, 128.47, 127.64, 127.62, 127.29, 127.26, 126.28, 126.26, 125.79, 125.77, 125.66, 125.64. HRMS ($C_{18}H_{12}S_2$): *m/z* 293.88 (M^+, calcd 292.03).

1,8-Bis(2,3-dihydrothieno[3,4-*b*][1,4]dioxin-5-yl)naphthalene (***o*-Np-EDOT)** was synthesized to the produce of *o*-Np-Th except using the EDOT-$SnBu_3$ to replace the Th-$SnBu_3$, and obtained faint yellow needle crystal with yield of 78.4%. ^1H NMR (500 MHz, $CDCl_3$), δ (TMS, ppm): 7.90–7.87 (m, 2H), 7.53–7.48 (m, 4H), 6.15 (s, 2H), 4.07 (s, 2H). ^{13}C NMR (125 MHz, $CDCl_3$) δ 140.41, 137.36, 134.77, 132.17. 131.30, 129.99,

129.34, 125.16, 117.25, 96.60, 64.41, 64.24. HRMS ($C_{22}H_{16}O_4S_2$): *m/z* 409.88 (M^+, calcd 408.04).

1,4-Bis(2,3-dihydrothieno[3,4-*b*][1,4]dioxin-5-yl)naphthalene (***p*-Np-EDOT)** was synthesized to the produce of *o*-Np-EDOT, and obtained faint yellow needle crystal with yield of 75.6%. ^{1}H NMR (500 MHz, $CDCl_3$), δ (TMS, ppm): 8.09–8.06 (m, 2H), 7.56 (s, 2H), 7.53–7.51 (m, 2H), 6.49(s, 2H), 4.29–4.21 (m, 8H). ^{13}C NMR (125 MHz, $CDCl_3$) δ 141.43, 138.36, 132.14, 130.51, 128.40, 126.73, 126.24, 115.18, 99.23, 64.71, 64.63. HRMS ($C_{22}H_{16}O_4S_2$): *m/z* 409.80 (M^+, calcd 408.04).

1,5-Bis(2,3-dihydrothieno[3,4-b][1,4]dioxin-5-yl)naphthalene (***m*-Np-EDOT)** was synthesized to the produce of *o*-Np-EDOT, and obtained faint yellow needle crystal with yield of 77%. ^{1}H NMR (500 MHz, $CDCl_3$), δ (TMS, ppm): 8.05 (d, J = 8.70 Hz, 2H), 7.57–7.56 (m, 2H), 7.53–7.50 (m, 2H), 6.48 (s, 2H), 4.29–4.26 (m, 4H), 4.23–4.21 (m, 4H). ^{13}C NMR (125 MHz, $CDCl_3$) δ 141.41, 138.27, 132.3, 130.27, 129.25, 127.08, 125.57, 115.44, 99.09, 64.73, 64.66. HRMS ($C_{22}H_{16}O_4S_2$): *m/z* 409.64 (M^+, calcd 408.04).

X-Ray Crystallography

Crystal data for ***p*-Np-Th** (CCDC 1902103): $C_{18}H_{12}S_2$, M_W = 292.4, orthorhombic, P 21 21 21, a = 5.92630 (10), b = 18.9112 (2), c = 24.8642 (3) Å, α = 90°, β = 90°, γ = 90°, V = 2786.62 (6) Å^3, Z = 8, D_c = 1.394, μ = 3.343 mm^{-1} (MoKa, λ = 1.54184), F(000) = 1216, T = 149.99 (10) K, $2\vartheta_{max}$ = 67.050° (100.00%), 96275 measured reflections, 4914 independent reflections (R_{int} = 0.0873), GOF on F^2 = 1.108, R_1 = 0.0576, wR_2 = 0.1695 (all data), Δe 0.967 and -0.580 eÅ^{-3}.

Crystal data for ***m*-Np-Th** (CCDC 1902101): $C_{18}H_{12}S_2$, M_W = 292.4, monoclinic, P 1 21/c 1, a = 8.6466 (3), b = 7.0684 (3), c = 11.6275 (5) Å, α = 90°, β = 94.936 (4) °, γ = 90°, V = 708.01 (5) Å^3, Z = 2, D_c = 1.372, μ = 3.267 mm^{-1} (MoKa, λ = 1.54184), F(000) = 304, T = 150.00 (10) K, $2\vartheta_{max}$ = 67.053° (100.00%), 2821 measured reflections, 1226 independent reflections (R_{int} = 0.0238), GOF on F^2 = 1.124, R_1 = 0.0607, wR_2 = 0.1411 (all data), Δe 0.640 and -0.490 eÅ^{-3}.

Crystal data for ***o*-Np-Th** (CCDC 1902102): $C_{18}H_{12}S_2$, M_W = 292.4, monoclinic, P 1 21/n

1, a = 10.9084 (2), b = 10.59026 (18), c = 12.3593(3) Å, α = 90°, β = 104.253 (2) °, γ = 90°, V = 1383.84 (5) Å^3, Z = 4, D_c = 1.403, μ = 3.343 mm^{-1} (MoKa, λ = 1.54184), F(000) = 608, T = 150.00 (10) K, $2\vartheta_{max}$ = 67.065° (100.00%), 9795 measured reflections, 2459 independent reflections (R_{int} = 0.0318), GOF on F^2 = 1.074, R_1 = 0.0320, wR_2 = 0.0824 (all data), Δe 0.274 and -0.276 eÅ^{-3}.

Crystal data for ***o*-Np-EDOT** (CCDC 1902107): $C_{22}H_{16}O_4S_2$, M_W = 408.47, orthorhombic, P c a 21, a = 8.19110 (10), b = 15.51400 (10), c = 14.1816 (2) Å, α = 90°, β = 90°, γ = 90°, V = 1802.15 (4) Å^3, Z = 4, D_c = 1.505, μ = 2.917 mm^{-1} (MoKa, λ = 1.54184), F(000) = 848, T = 149.99 (10) K, $2\vartheta_{max}$ = 67.684° (100.00%), 48774 measured reflections, 3392 independent reflections (R_{int} = 0.0329), GOF on F^2 = 1.030, R_1 = 0.0225, wR_2 = 0.0588 (all data), Δe 0.164 and -0.202 eÅ^{-3}.

Additional data

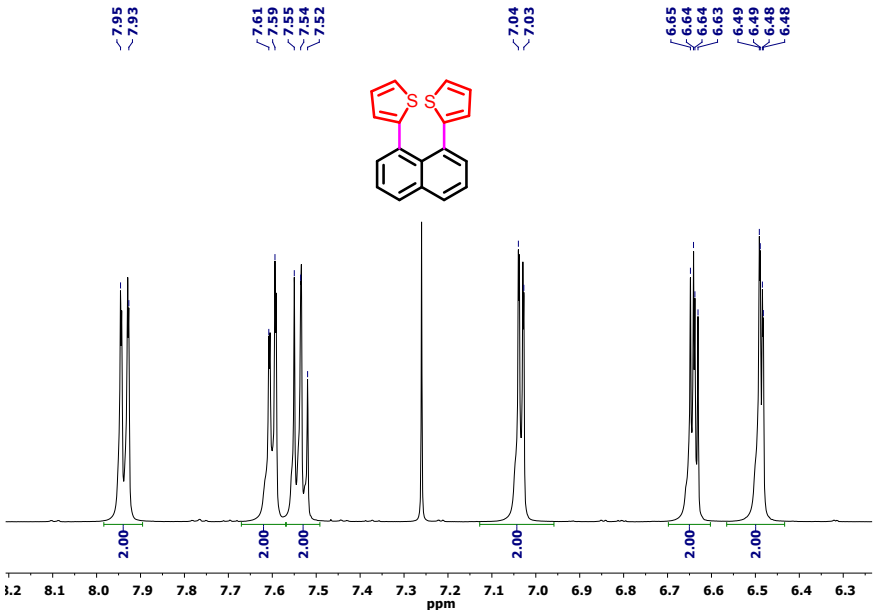

Fig. S2 ^{1}H NMR spectrum of compound ***o*-Np-Th** in $CDCl_3$.

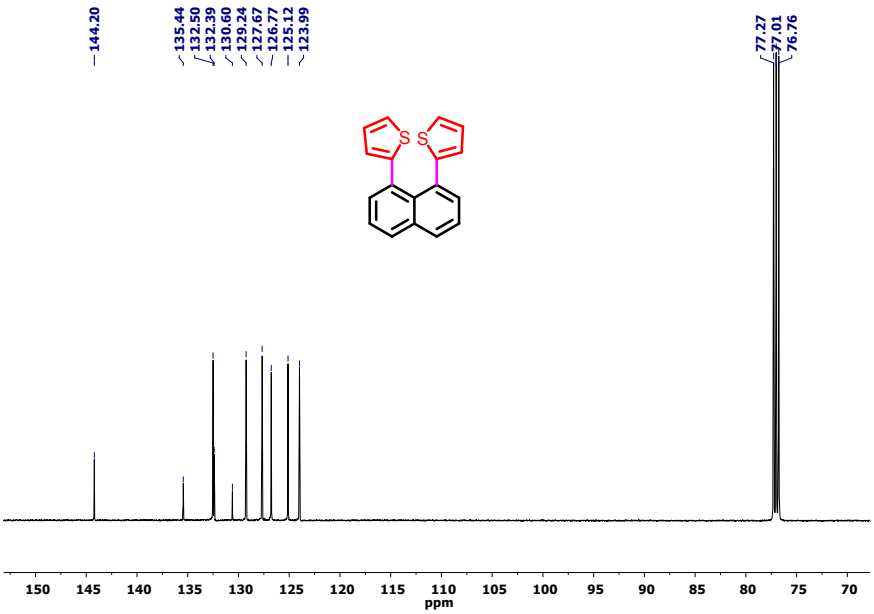

Fig. S3 ^{13}C NMR spectrum of compound ***o*-Np-Th** in $CDCl_3$.

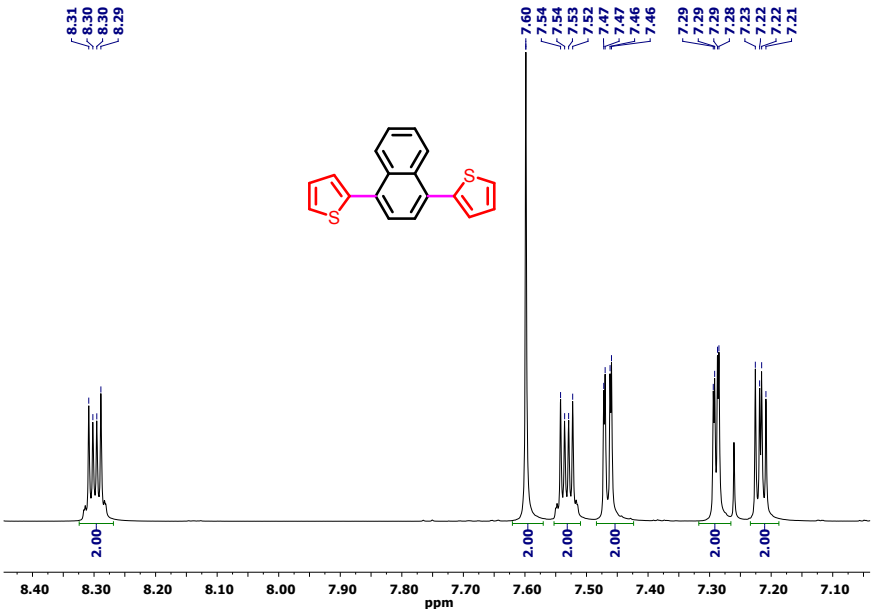

Fig. S4 ^{1}H NMR spectrum of compound ***p*-Np-Th** in $CDCl_3$.

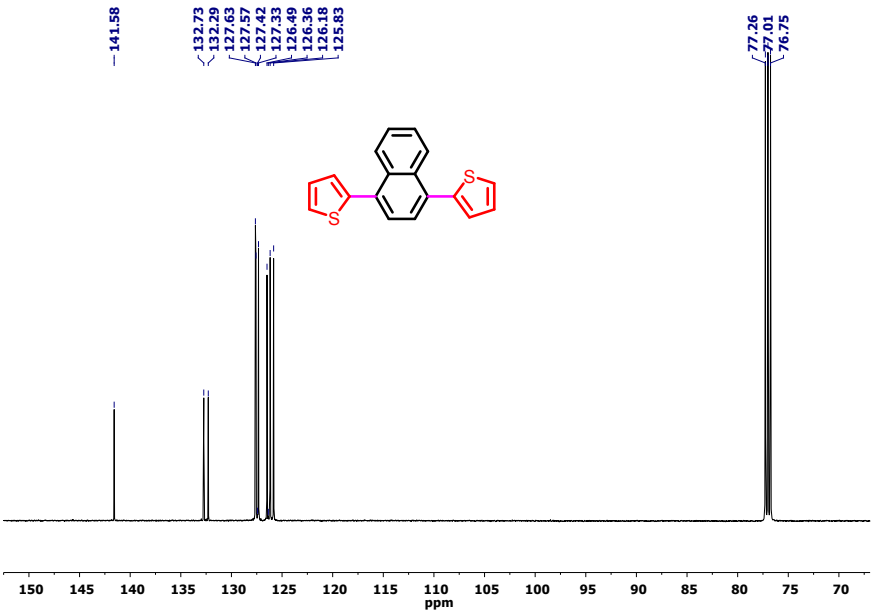

Fig. S5 ^{13}C NMR spectrum of compound ***p*-Np-Th** in $CDCl_3$.

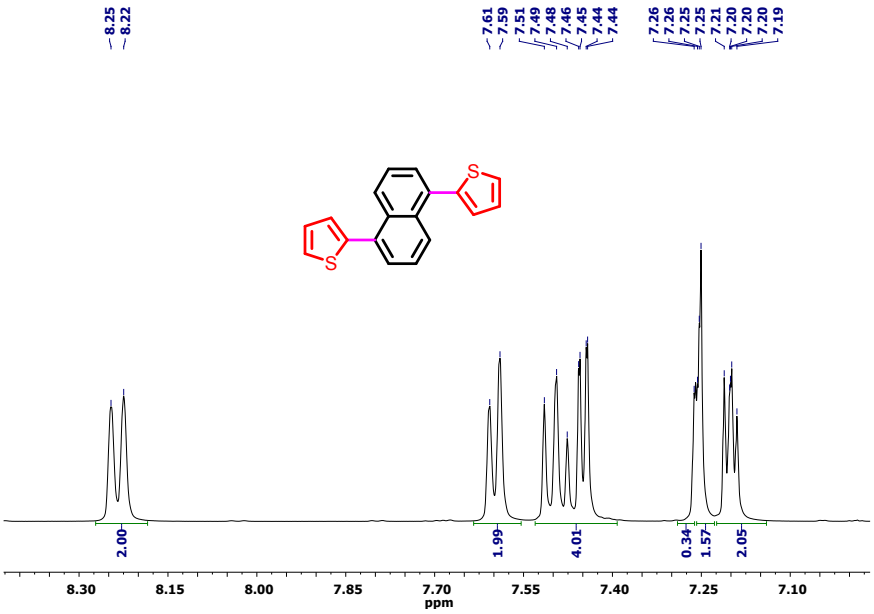

Fig. S6 ^{1}H NMR spectrum of compound ***m*-Np-Th** in $CDCl_3$.

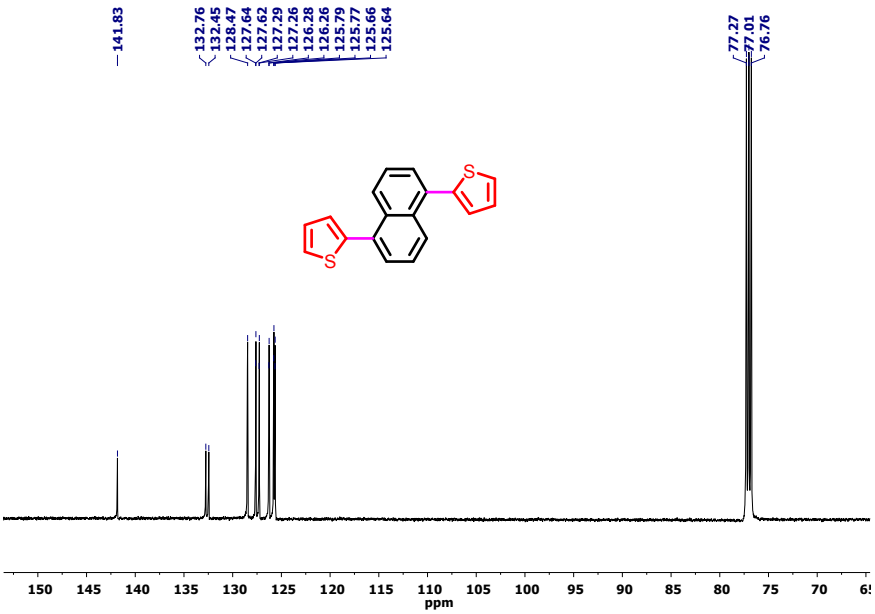

Fig. S7 ^{13}C NMR spectrum of compound ***m*-Np-Th** in $CDCl_3$.

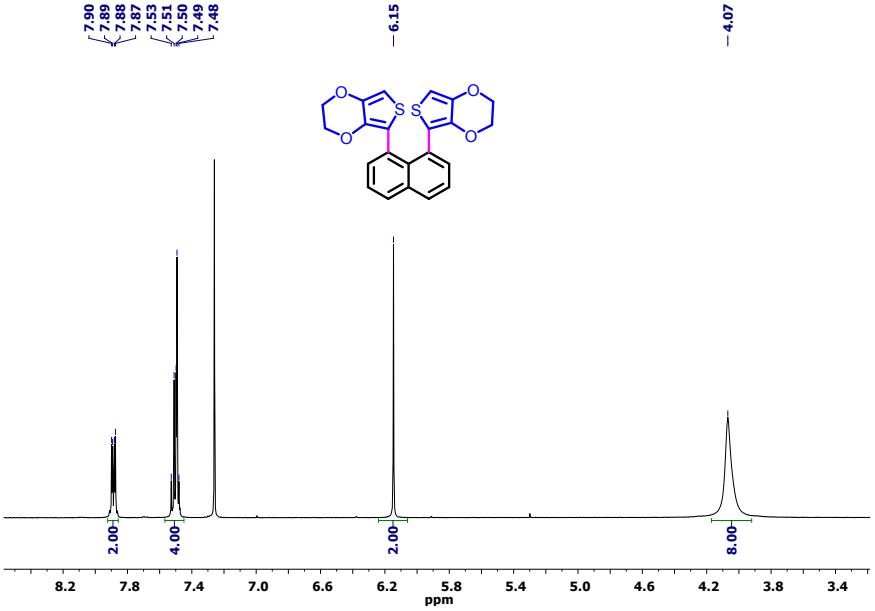

Fig. S8 ^{1}H NMR spectrum of compound ***o*-Np-EDOT** in $CDCl_3$.

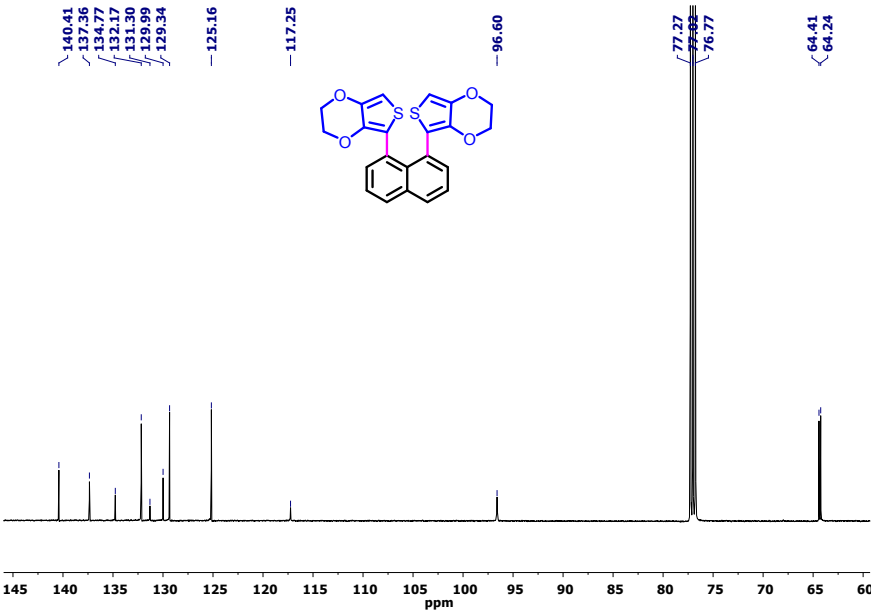

Fig. S9 ^{13}C NMR spectrum of compound ***o*-Np-EDOT** in $CDCl_3$.

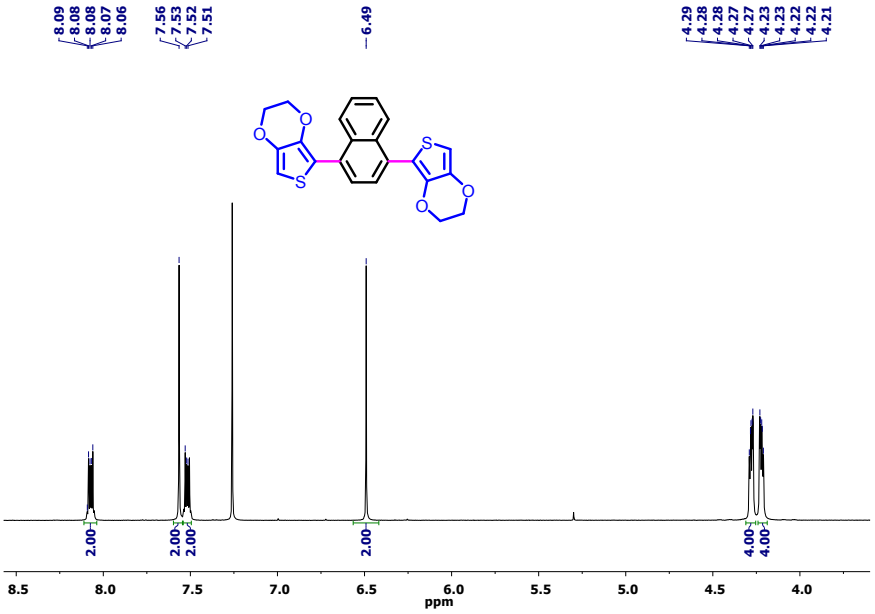

Fig. S10 ^{1}H NMR spectrum of compound ***p*-Np-EDOT** in $CDCl_3$.

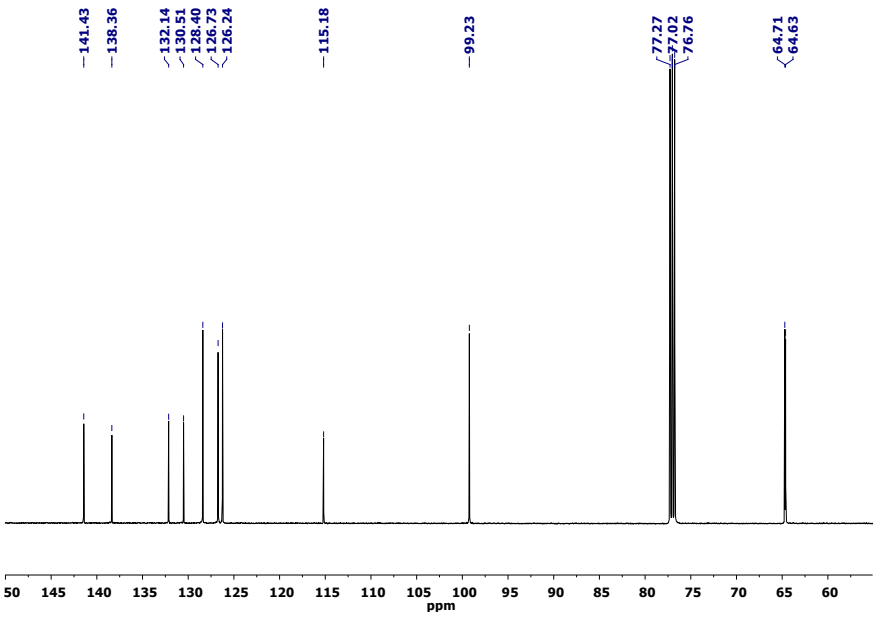

Fig. S11 ^{13}C NMR spectrum of compound ***p*-Np-EDOT** in $CDCl_3$.

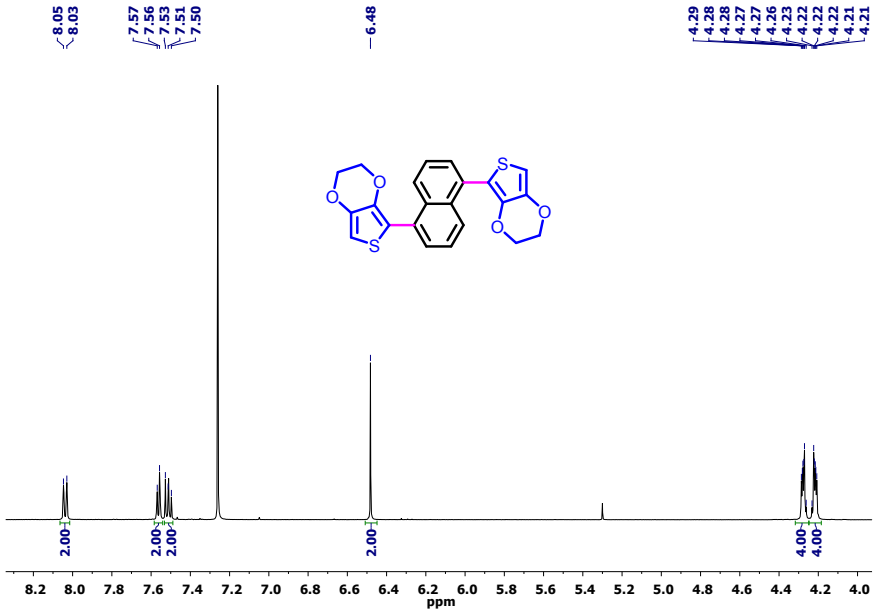

Fig. S12 ^{1}H NMR spectrum of compound ***m*-Np-EDOT** in $CDCl_3$.

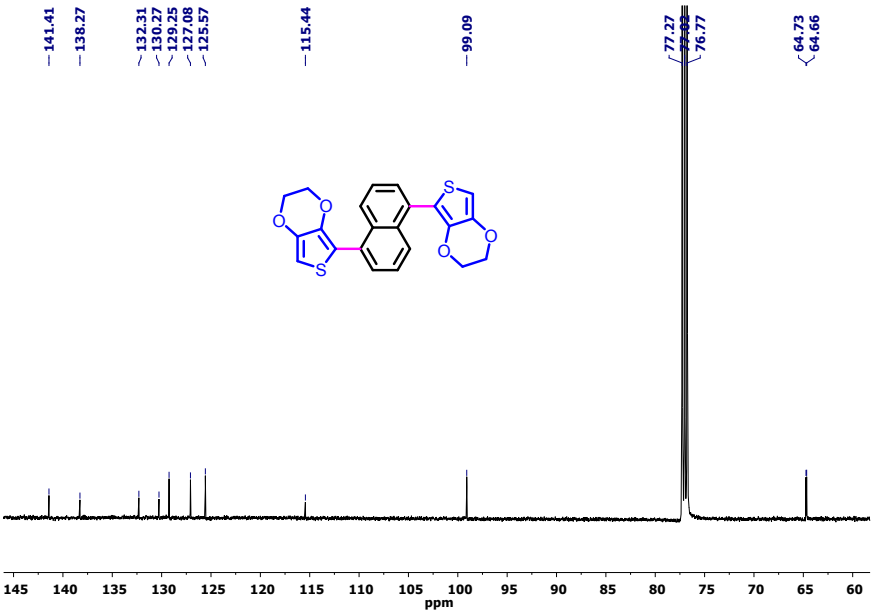

Fig. S13 ^{13}C NMR spectrum of compound ***m*-Np-EDOT** in $CDCl_3$.

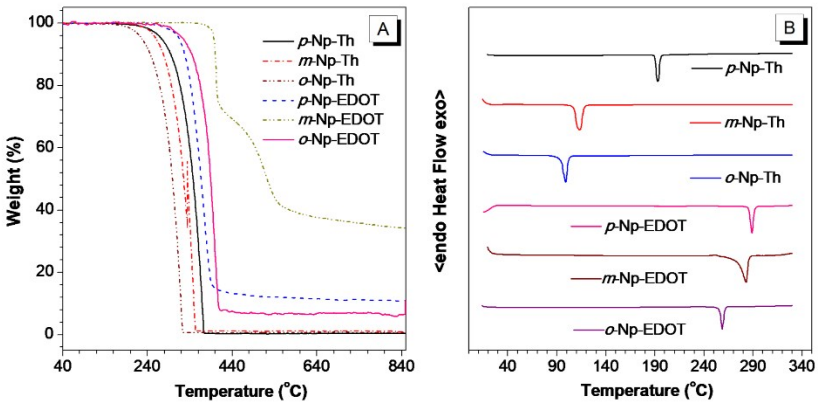

Fig. S14 TGA curves (A), DSC curves (B) of oligomers, recorded under nitrogen at a heating rate of 10 $^{o}C\ min^{-1}$.

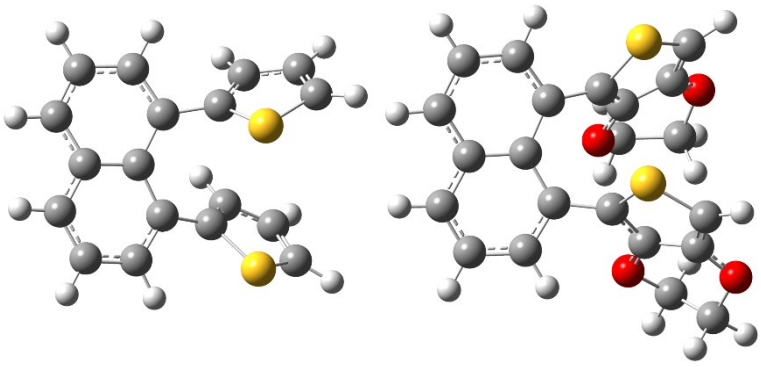

Fig. S15 Optimized anther configurations of ***o*-Np-Th** and ***o*-Np-EDOT.**

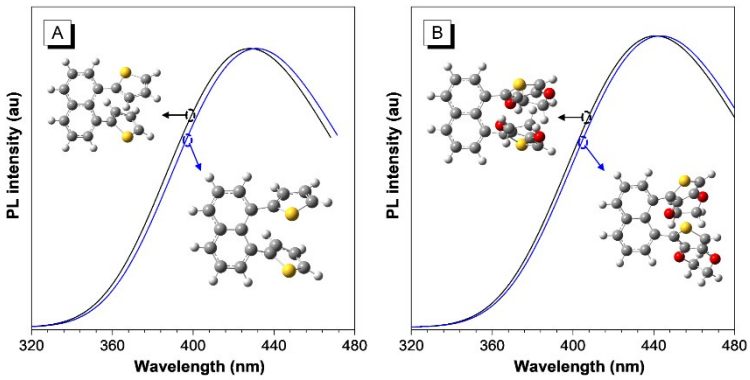

Fig. S16 Calculated PL spectra of ***o*-Np-Th** and ***o*-Np-EDOT** based on the optimized two configurations.

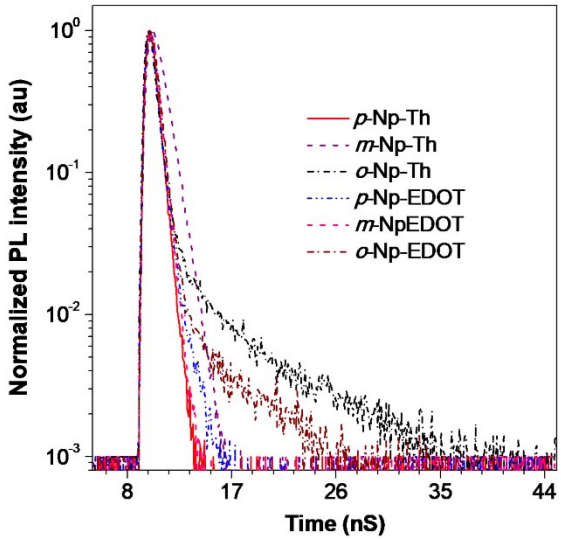

Fig. S17 PL decay curves of oligomers based on naphthalene.

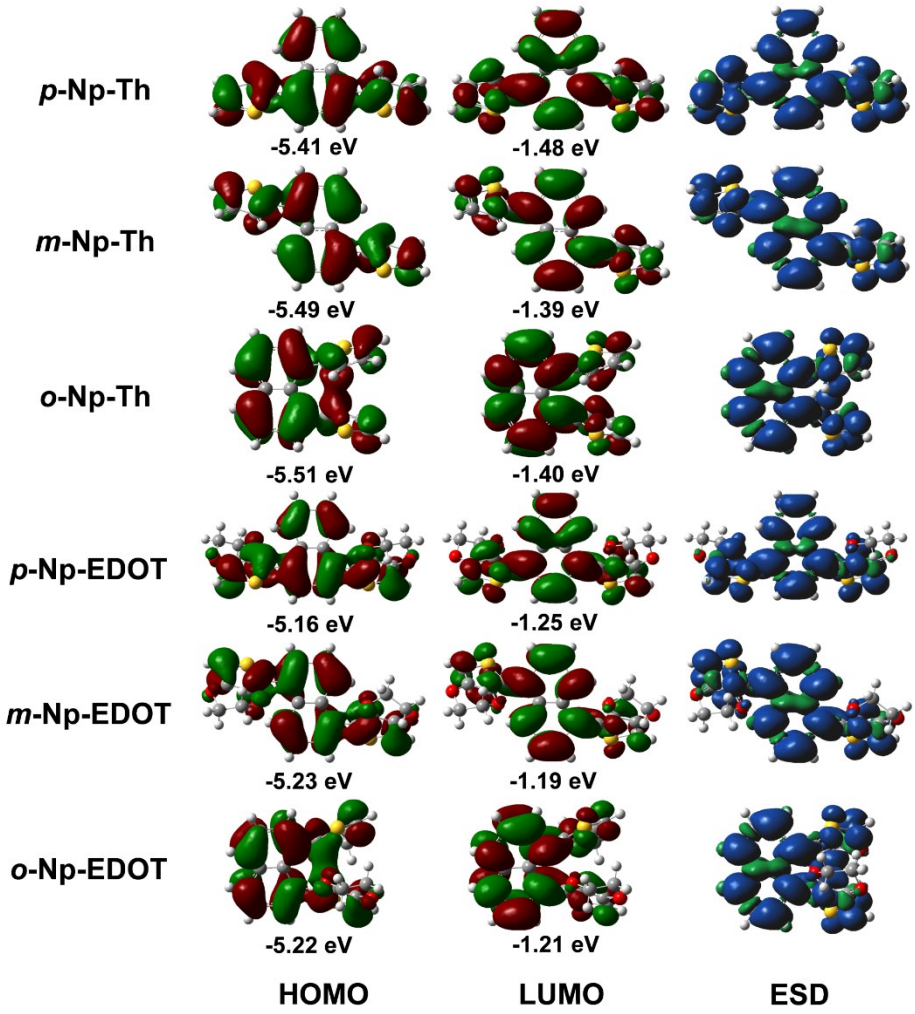

Fig. S18 Molecular frontier orbital amplitude plots of oligomers, isovalent surfaces of electron densities of radical cations of oligomers (C), calculated by B3LYP/6-31G(d, p).

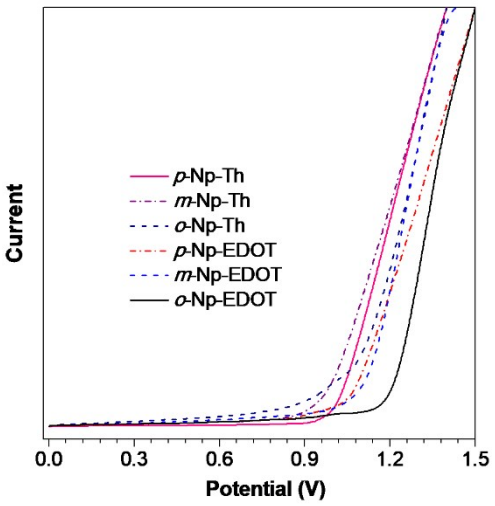

Fig. S19 Anodic oxidation curves of oligomers based on naphthalene.

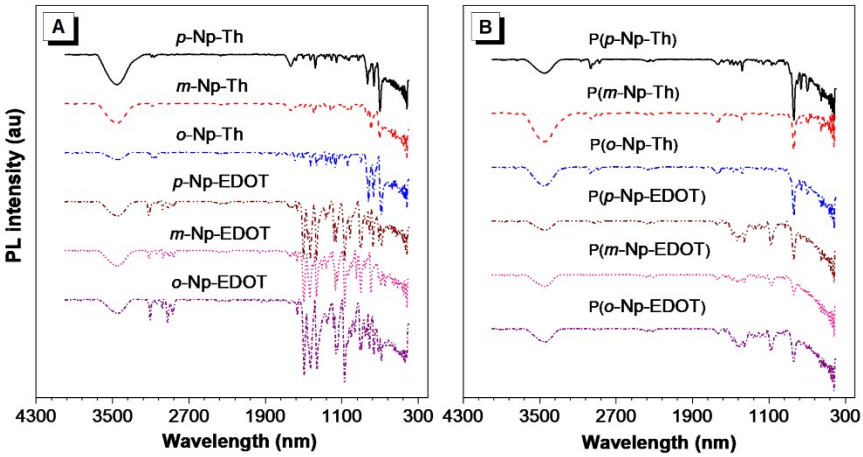

Fig. S20 FT-IR spectra of oligomers and polymers based on naphthalene.

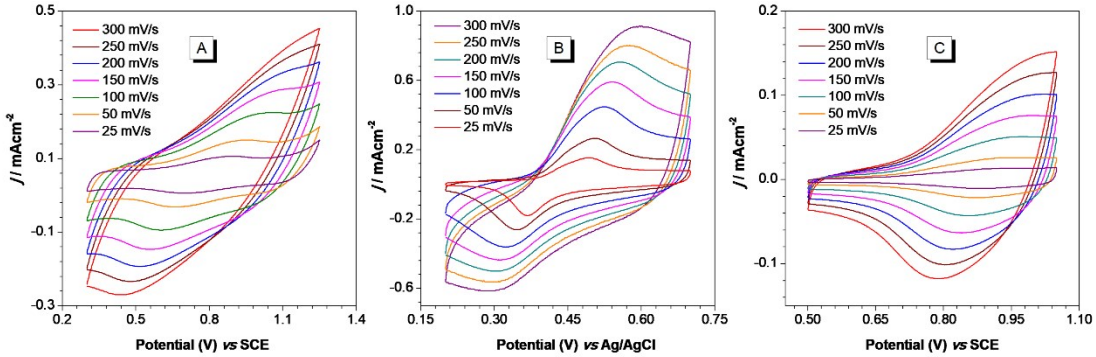

Fig. S21 CVs of **P(*m*-Np-Th)** (A), **P(*o*-Np-EDOT)** (B) and **P(*m*-Np-EDOT)** (C) in oligomer-free dichloromethane, containing 0.1 M Bu_4NPF_6. The potential scan rates are 300 mV/s, 250 mV/s, 200 mV/s, 150 mV/s, 100 mV/s, 50 mV/s and 25 mV/s, respectively.

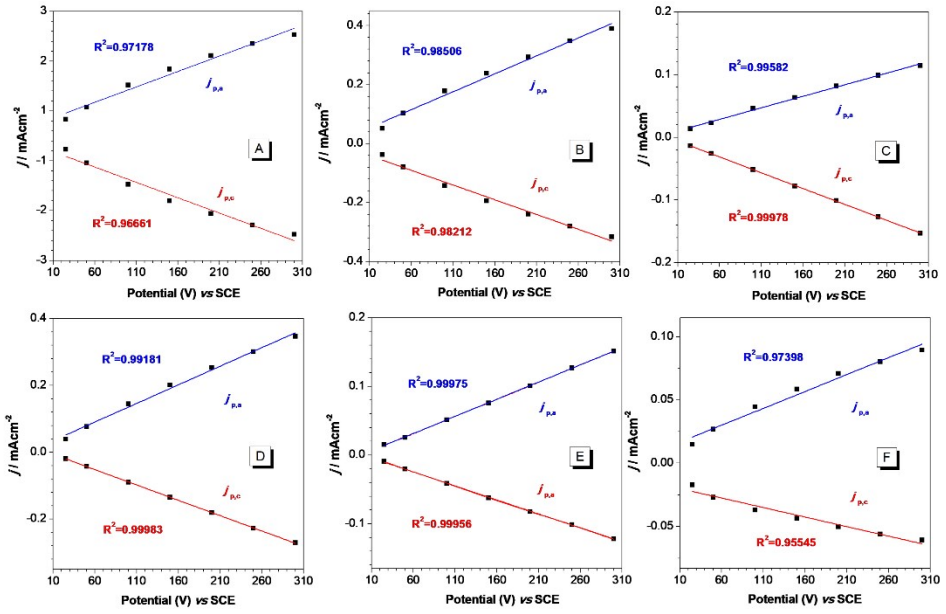

Fig. S22 Plots of redox peak current densities versus potential scan rates. And $j_{p,a}$ snd j_{pc} denote the anodic and cathodic peak current densities.

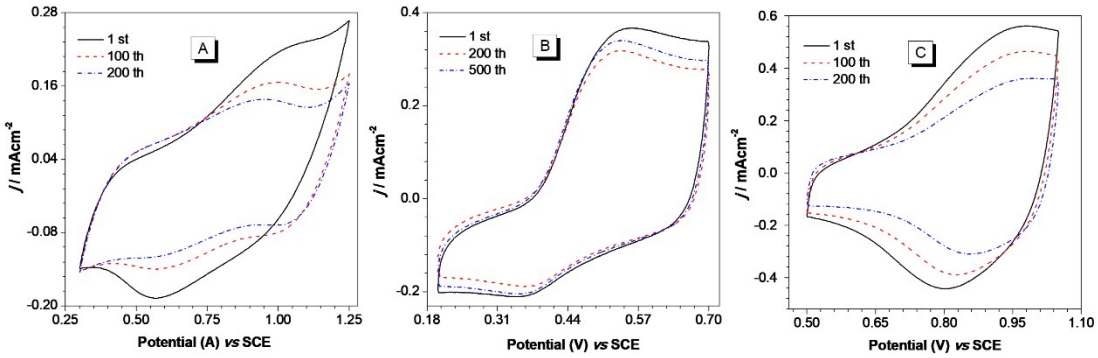

Fig. S23 Long-term redox stability of **P(*m*-Np-Th)** (A), **P(*o*-Np-EDOT)** (B) and **P(*m*-Np-EDOT)** (C) at the potential scan rate of 150 mV/s.

Reference

1 S. Ming, S. Zhen, X. Liu, K. Lin, H. Liu, Y. Zhao, B. Lu and J. Xu, *Poly. Chem.*, 2015, **6**, 8248-8258.